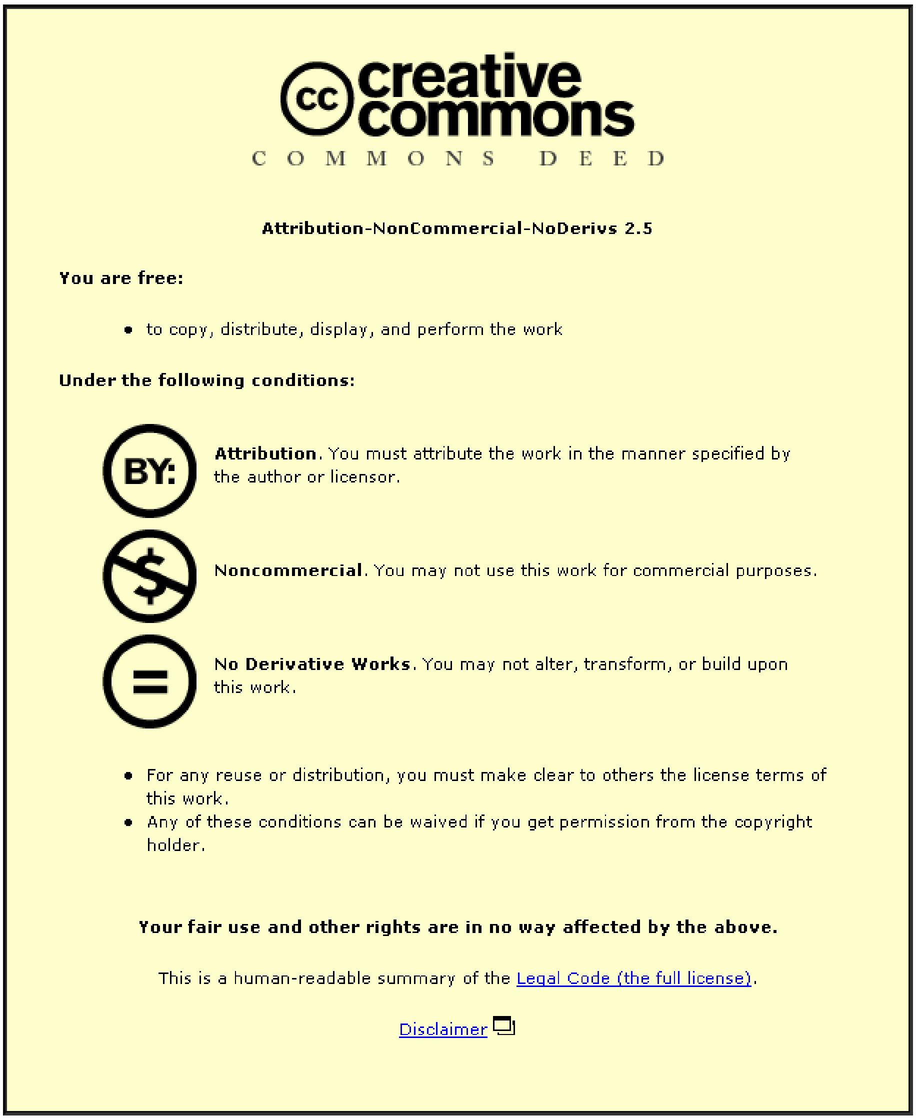

Measuring Pore Diameter Distribution of Gelcast Ceramic Foams from Two-Dimensional Cross Sections

Andrew M. Williams and Colin P. Garner

Wolfson School of Mechanical and Manufacturing Engineering, Loughborough University, Leicestershire LE11 3TU, UK

Jon G.P. Binner

Institute of Polymer Technology and Materials Engineering, Loughborough University, Leicestershire LE11 3TU, UK

Abstract: Increasing applications for gelcast ceramic foams is making the effective, accurate and cost effective measurement of pore diameter and distribution of significant value to a wide range of research fields. Current methods either do not directly measure pore diameter or they require high equipment and time costs. Measuring pore diameter directly from sample cross sections is both rapid and cost effective but, due to the random nature of the pore location during sectioning of the sample, it under predicts the pore diameter. The proposed method identified that the mean measured pore diameter was 79% (2 s.f.) of the actual pore diameter. Numerical methods for correcting the pore distribution as well as the average pore diameter are presented.

Keywords: *gelcast ceramic foam, pore diameter, rapid measurement, numerical methods*

Introduction

Porous materials offer advantages in many engineering applications including filtration, composite materials, catalysis, energy conversion and storage. Recent developments in porous ceramic manufacture[1,2] have resulted in the increasing application of gelcast ceramic foams[3,4,5,6,7] due to their improved strength and manufacturing characteristics when compared to ceramic foams made from other routes[8]. This increased strength is a result of the solid struts[1], shown in the image of a gelcast ceramic foam in Figure 1. The successful application of gelcast ceramic foams requires control of the porous structure, including the pore diameter. For example, the performance of gelcast ceramic foams in removing solid particulates from gas flow is highly dependent on the pore diameter of the foam[4]. The ability to rapidly, effectively and accurately measure the pore size of gelcast ceramic foams is, therefore, of interest to a wide range of engineering fields. This paper presents a method for accurately measuring the pore diameter from two-dimensional (2-D) cross sections of gelcast ceramic foams.

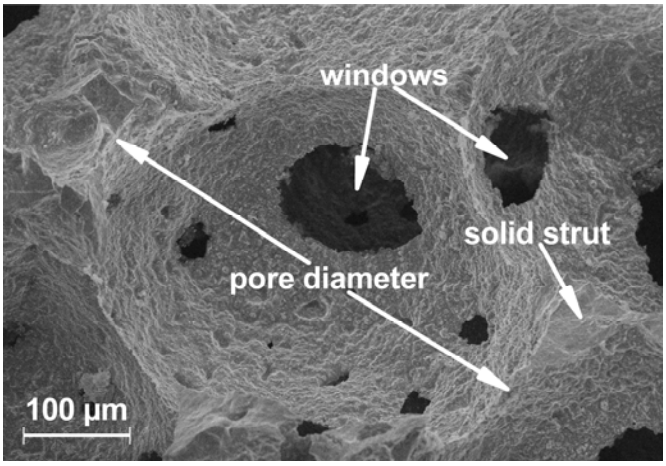

Figure 1 SEM image of gelcast ceramic foam

Pore diameter can be measured in a number of ways. Calibrated instruments can infer the pore diameter by applying a variable gas pressure to a liquid infiltrated porous sample (for example TRI/Princeton Autoporosimeter^{TM}). Direct spatial measurements can be made using three-dimensional (3-D) imaging techniques such as x-ray computer tomography (CT)[9] and nuclear magnetic resonance imaging[10,11] which require significant investment in time, equipment and resource. Techniques that can be performed in a general laboratory environment without the need for specialist equipment would support many fields of research using porous structures such as gelcast ceramic foams. Previous work with these materials has used optical measurement of sample cross sections to allow rapid and reliable comparison of different foam samples[1,4,12] using readily available and cost effective laboratory equipment. Due to the characteristics of sectioning a porous sample with predominantly spherical pores, statistically very few pores will be cut precisely at their diameter, resulting in a significant underestimate of the actual pore diameter of the foam sample. To use optical microscopy of gelcast foam cross sections to determine accurately the pore characteristics of the samples, an understanding of how the visible pore diameter is related to the actual pore diameter is required.

Although the work presented in this paper was independently derived, similar methods have been used in the metallography field for determining inclusion size characteristics[13]. The discretisation and geometric analysis developed by Saltykov (described in [14]) of sections through spherical inclusions allows quantitive measurements of 3-D microstructures in the same general form to the equations presented in this paper. The Saltykov method has been applied to low porosity foams[15] where the pores are isolated throughout the solid media to allow reconstruction of the foam 3-D microstructure. This communication presents a similar, independently derived method, for quantitively measuring pore size characteristics in gelcast ceramic foams, providing a tool for those working with gelcast ceramic foams to accurately quantify the foam characteristics.

Methodology

To understand the effect of the cutting plane, the gelcast geometry is simplified and considered as a single spherical pore, represented graphically in two dimensions in Figure 2. The cutting plane in this image is considered to be in the *y*-direction (i.e. constant *x*).

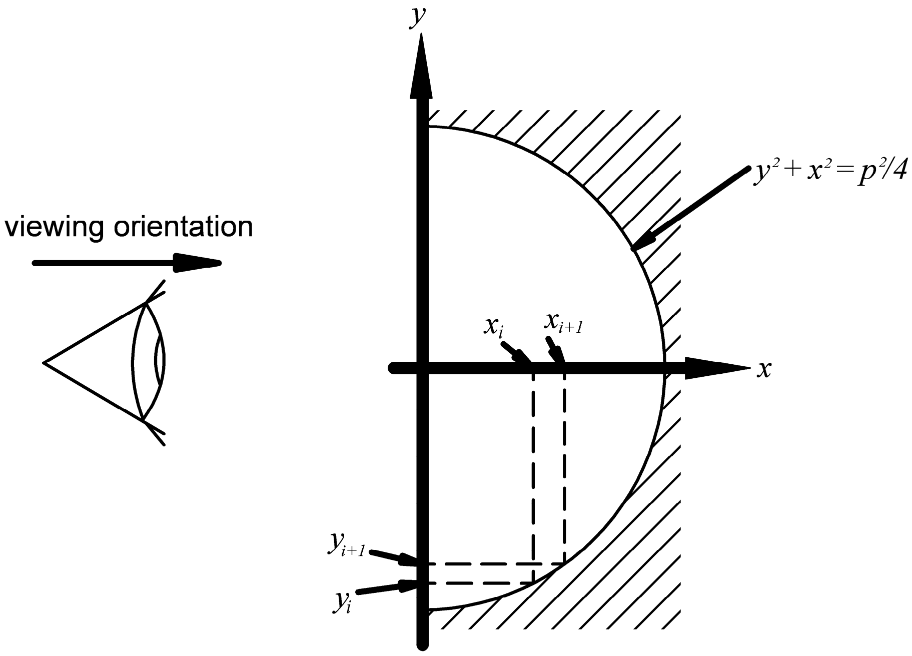

Figure 2 Graphical representation of the model of the random cutting plane for understanding the effect of the cutting plane position on the measurement of pore diameter

The probability of the cutting plane lying between the coordinates x_i and x_{i+1} is

$$P(x_i < x < x_{i+1}) = \frac{2(x_{i+1} - x_i)}{p} \tag{1}$$

where p is the actual pore diameter and x, x_i and x_{i+1} have the same meanings as in Figure 2. The factor of 2 comes from the symmetry of the pore around x=0. Since the relationship between x and y is known from the geometry of the pore, the probability of the visible radius being between y_{i+1} and y_i is the same as the probability of the cutting plane lying between x_i and x_{i+1}. This gives

$$P(y_{i+1} < y < y_i) = \frac{2\left[\left(\frac{p^2}{4} - y_{i+1}{}^2\right)^{0.5} - \left(\frac{p^2}{4} - y_i{}^2\right)^{0.5}\right]}{p} \tag{2}$$

The average visible pore size can be approximated by finding the probability for constant size intervals of y between 0 and $p/2$. As the interval size is reduced, the validity of this approximation increases. The ratio of the average measured pore size to the actual pore size is, therefore

$$\frac{p_{measured}}{p} = \frac{\sum_{i=1}^{(n-1)}\left[P(y_{i+1} < y < y_i)(y_i + y_{i+1})\right]}{p} \tag{3}$$

where n is the number of discreet intervals between $y=0$ and $2y=p$. The effect of interval size on the average measured pore diameter relative to the actual pore diameter is shown in Table 1. This demonstrates that as the interval size reduces, the mean visible pore diameter tends towards 79% (2 s.f.) of the actual pore diameter.

The number of measurements of visible pore diameter between y_{i+1} and y_i will be made from pores with diameters larger than the visible pore diameter such that the number of measurements will be

$$n_{y_{i+1}<y<y_i} = \sum_{j=1}^{m} n_i \frac{2}{p_i}\left[\left(\frac{p_i^{\,2}}{4} - y_{i+1}^{\,2}\right)^{0.5} - \left(\frac{p_i^{\,2}}{4} - y_i^{\,2}\right)^{0.5}\right] \qquad (4)$$

where n_i is the number of pores with a diameter p_i that would give n measurements of visible pore diameter between y_{i+1} and y_i. A series of simultaneous equations can be described that can be solved to find the original pore distribution. An example follows for the case of a system discretised into 10 sample ranges. The data is generated from a conceptual pore distribution where the visible pore distribution has been calculated from Equation (3) with discretisation interval of $p/250$. The simultaneous equations solved in matrix form, with constants calculated using Equation (4), are

$$\begin{bmatrix} 1 & 0.134 & 0.057 & 0.032 & 0.020 & 0.014 & 0.010 & 0.008 & 0.006 & 0.005 \\ 0 & 0.866 & 0.197 & 0.102 & 0.063 & 0.043 & 0.031 & 0.024 & 0.019 & 0.015 \\ 0 & 0 & 0.745 & 0.205 & 0.117 & 0.077 & 0.055 & 0.041 & 0.032 & 0.026 \\ 0 & 0 & 0 & 0.661 & 0.200 & 0.121 & 0.083 & 0.061 & 0.047 & 0.037 \\ 0 & 0 & 0 & 0 & 0.600 & 0.193 & 0.121 & 0.085 & 0.064 & 0.050 \\ 0 & 0 & 0 & 0 & 0 & 0.553 & 0.185 & 0.119 & 0.086 & 0.066 \\ 0 & 0 & 0 & 0 & 0 & 0 & 0.515 & 0.177 & 0.117 & 0.086 \\ 0 & 0 & 0 & 0 & 0 & 0 & 0 & 0.484 & 0.170 & 0.114 \\ 0 & 0 & 0 & 0 & 0 & 0 & 0 & 0 & 0.458 & 0.164 \\ 0 & 0 & 0 & 0 & 0 & 0 & 0 & 0 & 0 & 0.436 \end{bmatrix} \begin{bmatrix} n_{0<p<0.1} \\ n_{0.1<p<0.2} \\ n_{0.2<p<0.3} \\ n_{0.3<p<0.4} \\ n_{0.4<p<0.5} \\ n_{0.5<p<0.6} \\ n_{0.6<p<0.7} \\ n_{0.7<p<0.8} \\ n_{0.8<p<0.9} \\ n_{0.9<p<1} \end{bmatrix} = \begin{bmatrix} n_{0<p_{vis}<0.1} \\ n_{0.1<p_{vis}<0.2} \\ n_{0.2<p_{vis}<0.3} \\ n_{0.3<p_{vis}<0.4} \\ n_{0.4<p_{vis}<0.5} \\ n_{0.5<p_{vis}<0.6} \\ n_{0.6<p_{vis}<0.7} \\ n_{0.7<p_{vis}<0.8} \\ n_{0.8<p_{vis}<0.9} \\ n_{0.9<p_{vis}<1} \end{bmatrix} \tag{5}$$

Solving the matrix for the actual pore diameter gave the corrected pore distribution. Since this is a conceptual case, the actual pore distribution is known. Figure 3 shows the uncorrected pore distribution, the corrected pore distribution and the actual pore distribution for the above case. It shows that the correction is valid and it is noted that reducing interval size increased the validity of the correction.

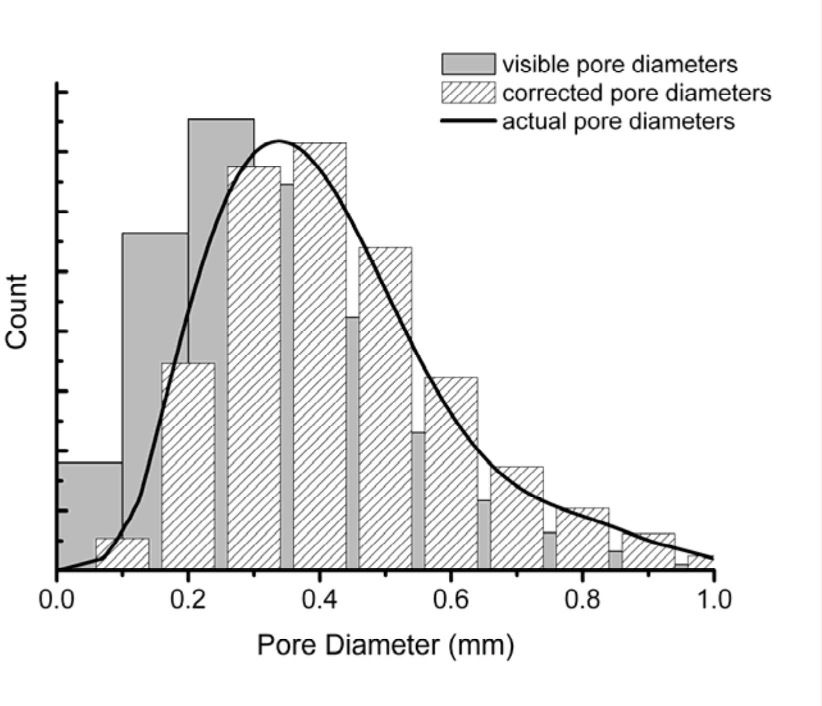

Figure 3 Pore distribution correction with 10 discretised ranges

Validation

To validate the proposed method a micro-CT scan of a sample gelcast ceramic foam was reconstructed, a part of which is shown in Figure 4. Pore diameter measurements of the sample were made from both a series of random 2-D cross sections and from the reconstructed 3-D image. The correction was applied to the sample to validate its use.

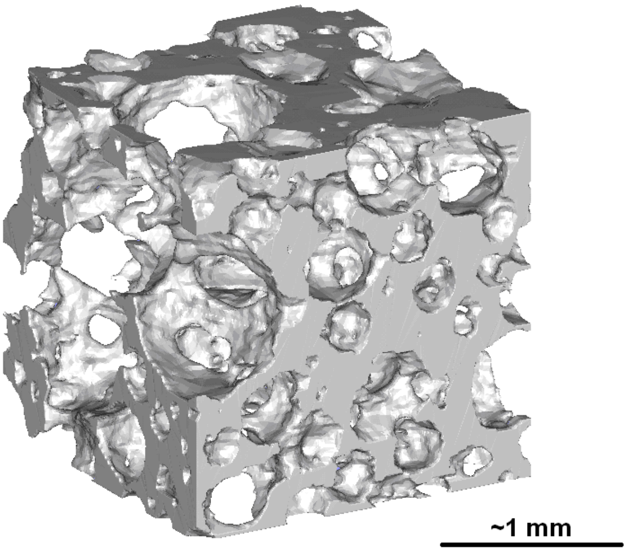

Figure 4 Reconstructed micro-CT scan of a sample of gelcast ceramic foam

The average visible diameter from the 2-D sections, the corrected average diameter (using the 0.79 factor) and the actual average diameter (from the 3-D measurements) were 165, 208 and 211 μm respectively for a sample size of 125 measurements. This shows the 0.79 factor is suitable for correcting the average pore diameter. Figure 5 shows the measured pore diameters from the 2-D cross sections (the visible diameters), the corrected distribution and the measured pore diameters from the 3-D reconstruction (the actual pore diameters). When applying the correction, the distribution tends to shift to the larger pore sizes as previously discussed. This shows that the correction of the distribution measured from 2-D cross sections is very effective. The magnitude in the plot is different due to the different number of samples taken and is not a result of the correction methodology.

Figure 5 Curve fit data to allow easy comparison of the pore distribution for each of the measurement methods

Sample Size Considerations

The sample size has a significant effect on the potential errors. Approximating the population as a log-normal distribution and using a t-distribution analysis of the transformed idealised data (used earlier), an estimation of the confidence intervals of the 0.79 correction factor were found. The effect of sample size on the confidence intervals is shown in Figure 6. It is clear that sample sizes >100 are reasonable, although this would depend on the field and application of the foam under investigation. Confidence intervals can be determined in this way for specific samples and measurements.

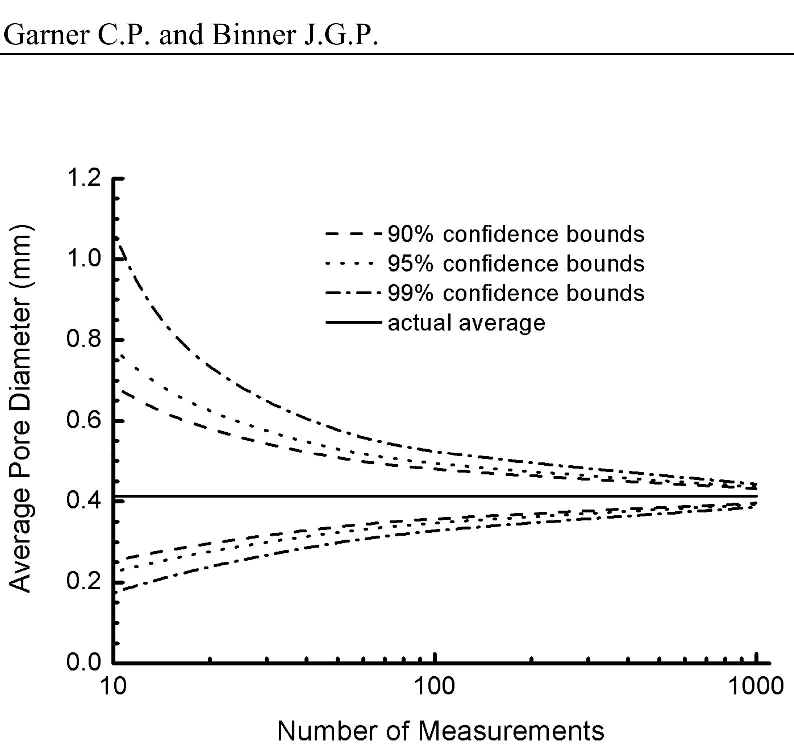

Figure 6 Effect of number of measured diameters on the confidence intervals for an example measurement of average pore diameter

The discretised pore distribution must be smooth the get a reasonable converted distribution. Intervals with very low number counts can lead to negative numbers once converted using Equation (4). This, however can be overcome by reducing the number of intervals (i.e. increasing the interval size) to smooth out the measured distribution.

Summary and Conclusions

Rapid, cost effective and accurate methodology is needed for measurement of the pore size and distribution of gelcast ceramic foams. The direct measurement of pore diameter from 2-D cross sections of foam structures yields an underestimate of the actual pore diameter. This research has developed and applied methods for using the 2-D cross sections to accurately measure pore diameter and distribution showing:

1. The average pore diameter can be found by dividing the visible average pore diameter on the 2-D cross section by 0.79 (2 s.f.).
2. Numerical methods have been developed and described that allow the pore distribution to be corrected for the underestimate of pore size when measuring visible pore size from 2-D cross sections.
3. The methodology has been demonstrated by means of an example distribution and has been applied to a real world case as validation of the method. This validation showed the described method to be very effective for correcting the pore diameter and distribution.
4. An example case has been used to indicate the confidence intervals and effects of sample size on determining the average pore diameter. A typical sample size would be >100 measurements, although would vary depending on the application.

References

[1.] P. Sepulveda and J.G.P. Binner, "Processing of cellular ceramics by foaming and in situ polymerisation of organic monomers," *J. Eur. Ceram. Soc.*, 19, 2059-2066 (1999)

[2.] J.G.P. Binner, "Gel casting of ceramic foams," *Proceedings of the 27th Annual International Conference and Exposition on Advanced Ceramics and Composites, Cocoa Beach, Florida, January 2003*

[3.] P. Sepulveda, J.G.P. Binner, S.O. Rogero, O.Z. Higa and J.C. Bressiani, "Production of porous hydroxyapatite by the gel-casting of foams and cytotoxic evaluation," *J. of Biomed. Mater. Res.,* 50 [1] 27-34 (2000)

[4] S.W. Hughes (2003) The use of gel cast ceramic foams as diesel particulate filters. *PhD Thesis – Loughborough University, UK* (2003)

[5] R. Mouazer, I. Thijs, S. Mullens and J. Luyten, "SiC foams produced by gel casting: synthesis and characterisation," *Adv. Eng. Mater.,* 6 [5] 340-343 (2004)

[6] J.G.P. Binner, S. Hughes and R.M. Sambrook "Gel cast foam diesel particulate filters," *Key Eng. Mater.,* 264-268 [III], *Euro Ceramics VIII,* 2231-2234 (2004)

[7] R.L. Menchavez, M. Fuji, H. Takegami and M. Takahashi, "Electrically conductive gelcast porous alumina sintered under argon atmosphere," *Mater. Lett.,* 61 754-756 (2007)

[8] M. Scheffler (Ed) and P. Colombo (Ed) Cellular Ceramics. *Wiley-VCH, Weinheim, Germany, ISBN 978-3527313204*

[9] O.B. Olurin, M. Arnold, C. Körner and R.F. Singer, "The investigation of morphometric parameters of aluminium foams using micro-computed tomography," *Mater. Sci. Eng.,* A328 334-343 (2002)

[10] J.H. Strange, M. Rahman and E.G. Smith, "Characterization of porous solids by NMR," *Physic. Rev. Lett.,* 71 [21] 3589-3591 (1993)

[11] J.H. Strange J.H. and J.B.W. Webber, "Spatially resolved pore size distributions by NMR," *Meas. Sci. Technol.,* 8 555-561 (1997)

[12] E.M. Adigio, "Modelling gas flow pressure gradients in gelcast ceramic foam diesel particulate filters," *PhD Thesis – Loughborough University, UK (2005)*

[13] J. Gegner, "2D-3D Conversion of Object Size Distributions in Quantitative Metallography," *Proceedings of the MMT-2006 conference*, pp.3/109-120, Ariel, Israel,11-15, September (2006).

[14.] R.T. DeHoff (Ed) and F.N. Rhines (Ed), “Quantitative Microscopy,” McGraw-Hill Inc, New York, (1968)

[15.] H. Shen, S.M. Oppenheimer, D.C. Dunand, L.C. Brinson, “Numerical modelling of pore size distribution in foamed titanium,” *Mech. Mater.* 38 933-944 (2006)

Nomenclature:

n_i	number of pores of diameter p_i that would generate the visible pore distribution
$n_{y1<y<y2}$	number of pores with visible diameter in the range $y1<y<y2$
p	pore diameter
$P(\ldots)$	probability of (…)
x	spatial position
y	spatial position

Figure Captions:

Figure 1 SEM image of gelcast ceramic foam

Figure 2 Graphical representation of the model of the random cutting plane for understanding the effect of the cutting plane position on the measurement of pore diameter

Figure 3 Pore distribution correction with 10 discretised ranges

Figure 4 Reconstructed micro-CT scan of a sample of gelcast ceramic foam

Figure 5 Curve fit data to allow easy comparison of the pore distribution for each of the measurement methods

Figure 6 Effect of number of measured diameters on the confidence intervals for an example measurement of average pore diameter

Tables:

Table 1 Effect of interval size on the calculation of the correction factor for the measured pore size.

Interval Size	Mean Measured Diameter/Actual Diameter
$p/10$	0.7593
$p/20$	0.7761
$p/40$	0.7821
$p/100$	0.7846
$p/1000$	0.7854